Imino proton exchange and base-pair kinetics in the AMP-RNA aptamer complex

Sylvie Nonin, Feng Jiang, Dinshaw Patel

Imino Proton Exchange and Base-pair Kinetics in the AMP–RNA Aptamer Complex

Sylvie Nonin*, Feng Jiang and Dinshaw J. Patel

Cellular Biochemistry & Biophysics Program, Memorial Sloan-Kettering Cancer Center New York, NY 10021, USA

We report on the dynamics of base-pair opening in the ATP-binding asymmetric internal loop and flanking base-pairs of the AMP–RNA aptamer complex by monitoring the exchange characteristics of the extremely well resolved imino protons in the NMR spectrum of the complex. The kinetics of imino proton exchange as a function of basic pH or added ammonia catalyst are used to measure the apparent base-pair dissociation constants and lifetimes of Watson–Crick and mismatched base-pairs, as well as the solvent accessibility of the unpaired imino protons in the complex. The exchange characteristics of the imino protons identify the existence of four additional hydrogen bonds stabilizing the conformation of the asymmetric ATP-binding internal loop that were not detected by NOEs and coupling constants alone, but are readily accommodated in the previously reported solution structure of the AMP–RNA aptamer complex published from our laboratory. The hydrogen exchange kinetics of the non-Watson–Crick pairs in the asymmetric internal loop of the AMP–RNA aptamer complex have been characterized and yield apparent dissociation constants (αK_d) that range from 10^{-2} to 10^{-7}. Surprisingly, three of these αK_d values are amongst the lowest measured for all base-pairs in the AMP–RNA aptamer complex. Comparative studies of hydrogen exchange of the imino protons in the free RNA aptamer and the AMP–RNA aptamer complex establish that complexation stabilizes not only the bases within the ATP-binding asymmetric internal loop, but also the flanking stem base-pairs (two pairs on either side) of the binding site. We also outline some preliminary results related to the exchange properties of a sugar 2′-hydroxyl proton of a guanosine residue involved in a novel hydrogen bond that has been shown to contribute to the immobilization of the bound AMP by the RNA aptamer, and whose resonance is narrow and downfield shifted in the spectrum.

Keywords: AMP–RNA aptamer complex; imino proton exchange; base-pair dissociation constants; mismatch pair opening; sugar 2′-OH groups

**Corresponding author*

Introduction

Base-pairing plays a key role in the structure, interactions and function of nucleic acids. The majority of NMR-based structural approaches have focused on the pairing alignments deduced from the characterization of nucleic acid structures in solution. An important complement to this structural information is provided by NMR-based hydrogen exchange measurements of imino protons in nucleic acids, which provide a measure of the kinetics of base-pair opening at the individual base-pair level. The strength of the imino proton exchange method lies in its ability to probe the structure and detect local anomalies at the base-pair level without assumptions on the folding or the pairing topology. The most striking result provided by this approach to date was the discovery of the four-stranded *i*-motif DNA (Gehring *et al.*, 1993; Leroy *et al.*, 1993) in which imino proton exchange played a determinant role. Much of the early NMR-based structural and hydrogen exchange research has focused on *B*-DNA duplexes

Permanent address: S. Nonin, BIOP-Ecole Polytechnique, 91129 Palaiseau, France.

Abbreviations used: JR, jump-and-return; NOE, nuclear Overhauser effect; NMR, nuclear magnetic resonance; ppm, parts per million; FID, free induction decay; N, any base; R, purine.

containing Watson–Crick base-pairs and occasional helical errors such as bulges and mismatches, which can be readily studied by their characteristic signatures in the NMR spectra. By contrast, RNA with its additional 2′-OH group is capable of adopting novel tertiary folds stabilized by unusual pairing alignments. The kinetics of imino proton exchange has the potential of monitoring which imino protons are base-paired, and which are not in the folded RNA tertiary structure, and has the potential for providing an independent probe of structural properties without any assumption concerning the conformation of the molecule.

NMR-based imino proton exchange and the kinetics of opening at the individual base-pair level have been developed in the Guéron laboratory with the methodology and applications reviewed by this group (Guéron *et al.*, 1989; Guéron & Leroy, 1995). It is approached by interpreting the imino proton exchange with water under the catalysis of proton acceptors with the corresponding exchange at the mononucleoside level, which provides the benchmark for analysis of the exchange data. The apparent dissociation constants for base-pair opening are derived from the comparison of the exchange catalysis by external acceptors such as hydroxide or ammonia. Base-pair lifetimes are obtained as the limit of the imino proton exchange time under infinite concentration of catalyst. In addition, intrinsic catalysis is a process specific to an imino proton engaged in a pair and can yield information about the geometry of the open state (Guéron *et al.*, 1987).

Such imino proton hydrogen exchange and base-pair opening studies have been conducted previously on *B*-DNA (Kochoyan *et al.*, 1987; Leroy *et al.*, 1988b; Nonin *et al.*, 1995, 1996; Folta-Stogniew & Russu, 1996), *A*-tract DNA (Leroy *et al.*, 1988a; Moe & Russu, 1990; Maltseva *et al.*, 1993; Guéron & Leroy, 1995; Moe *et al.*, 1995), Z-DNA (Kochoyan *et al.*, 1990), the *i*-motif formed by intercalated $C \cdot C^+$ base-pairs (Leroy *et al.*, 1993; Nonin *et al.*, 1996) and drug–DNA complexes (Leroy *et al.*, 1991, 1992). By contrast, fewer imino proton hydrogen exchange studies have been conducted on RNA and to date have been restricted to oligomeric duplexes (Fritzche *et al.*, 1983), synthetic polymers poly(rA)·poly(rU) and poly(rI)·poly(rC) (Leroy *et al.*, 1985b), yeast $tRNA^{Phe}$ and $tRNA^{Asp}$ (Leroy *et al.*, 1985a) and *Escherichia coli* 5 S RNA and its complex with the L5 protein (Leontis & Moore, 1986). Recently, the method has also been applied to the study of a DNA–RNA hybrid duplex (Maltseva *et al.*, 1995).

A novel RNA secondary structure containing an asymmetric internal loop has been identified to bind tightly to the universal energy cofactor ATP (and its analog AMP) from in vitro selection experiments (Sassanfar & Szostak, 1993). The asymmetric internal loop contains a conserved 11-base purine-rich segment positioned opposite an invariant guanine with this domain constituting the ATP binding site (Figure 1(a)). Two groups have

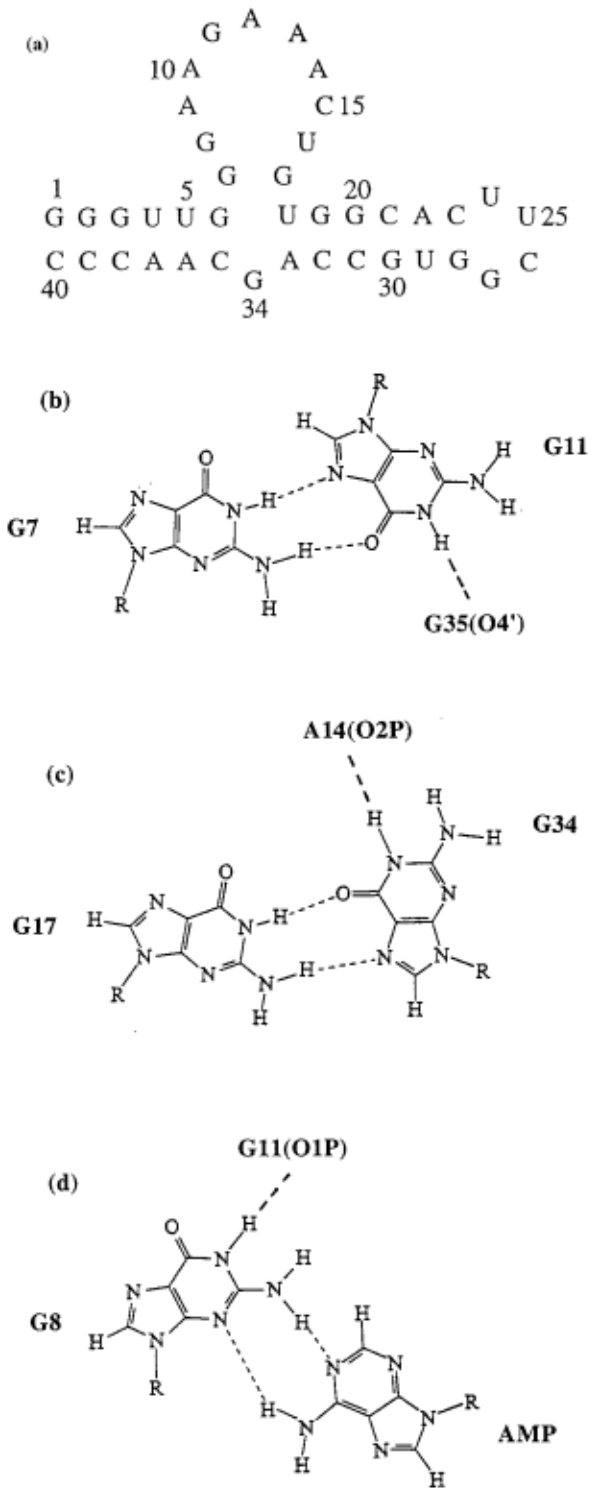

Figure 1. (a) Sequence and numbering system of AMP-binding 40-nucleotide RNA aptamer. Residues 1 to 6 and 35 to 40 are part of the left stem, residues 18 to 23 and 28 to 33 of the right stem. The ATP-binding asymmetric internal loop encompasses residues 7 to 17 and 34. A stable UUCG hairpin loop spans residues 24 to 27. Schematics outlining hydrogen bonding alignments for: (b) the G7·G11 mismatch, (c) the G17·G34 mismatch and (d) the intermolecular G8·AMP interaction in the AMP–RNA aptamer complex. We also show potential hydrogen bond acceptors for the imino protons G11, G34 and G8 in the complex.

recently characterized the solution structure of an AMP–RNA aptamer complex based on a combined NMR and molecular dynamics study (Jiang *et al.*, 1996a; Dieckmann *et al.*, 1996). The AMP–RNA aptamer complex adopts an L-shaped structure with two nearly orthogonal stems projecting away from the cofactor binding site. The purine ring of AMP intercalates between A10 and G11 with the G8-A9-A10-AMP segment folding into a GNRA-like motif in the complex. The ATP-binding loop folds into two distinct hairpins that form a network of non-Watson–Crick base-pairing and stacking interactions that enclose the AMP within the binding pocket. The present study characterizes the imino proton hydrogen exchange in the AMP–RNA aptamer complex with special emphasis on the exchange characteristics of imino protons in the asymmetric internal loop and flanking Watson–Crick stem base-pairs.

We have characterized the imino proton exchange properties and the stability of base-pair mismatches (Figures 1(b), (c) and (d)) in the RNA binding loop of the AMP–RNA aptamer complex and compared the base-pair opening kinetics with what is commonly observed in DNA. The six imino protons in the ATP-binding asymmetric internal loop (including G34) are subject to intrinsic catalysis in the AMP–RNA aptamer complex, which allows the identification of four additional hydrogen bonds (beyond those outlined in the Jiang *et al.*, 1996a structural study) that contribute to the stabilization of the structure. The present study establishes that RNA can accommodate base-pair mismatches within its global fold that are more stable than their corresponding Watson–Crick aligned counterparts. It also establishes that the theory developed thus far to explain the exchange properties of imino protons in Watson–Crick base-pairs also accounts for the exchange properties of imino protons in Hoogsteen and reversed-Hoogsteen mismatched base-pairs. Comparative imino proton exchange experiments undertaken on the free 40-mer RNA aptamer and its AMP complex establishes that complex formation stabilizes both the bases within the asymmetric binding loop and the flanking stem base-pairs (two each on either side) in the complex. We have also obtained preliminary exchange data concerning the downfield-shifted narrow resonance (9.4 ppm) originating in the sugar 2′-OH proton of G34 in the AMP–RNA aptamer complex.

Theory

The theory of imino proton exchange has been reviewed (Guéron *et al.*, 1989; Guéron & Leroy, 1995) and its salient features relevant to the present study are summarized below. Imino proton exchange from a base-pair requires two successive steps involving initial base-pair opening followed by exchange from the open state (Leroy *et al.*, 1985b). Exchange from the closed base-pair is either forbidden or very inefficient and includes the case where the imino proton in the pair is exposed to solvent (Nonin *et al.*, 1995). The exchange is catalyzed by the presence of proton acceptors with the catalysts being either external (NH_3, phosphate, OH^-), or intrinsic (the acceptor of the imino proton hydrogen bond; N^3 of C in G·C and N^1 of A in A·T Watson–Crick base-pairs) (Guéron *et al.*, 1987). Several catalysts may coexist in solution.

External catalysis

External catalysis acts on every kind of imino proton with similar exchange properties in the open state and in the monomer:

$$k_{ex,acc,open} = \alpha k_{ex,acc} \tag{1}$$

with

$$k_{ex,acc} \approx q_{acc}[acc]\ 10^{pK_{acc}-pK_i} \tag{2}$$

where the exchange rates $k_{ex,acc,open}$ and $k_{ex,acc}$ refer to the open state and to the monomer, respectively, and where α summarizes any difference between the case of the monomer and that of the open state. The factor α was shown not to be strongly catalyst-sensitive and not too far from unity (Guéron *et al.*, 1989). pK_{acc} and pK_i are the pK of, respectively, the external acceptor and the nucleic acid imino proton. q_{acc} stands for the collision constant and [acc] is the concentration of the basic form of the catalyst.

When OH^- is the acceptor, equation (2) becomes:

$$k_{ex,OH^-} = q_{OH^-}\ 10^{pH-pK_i} \tag{3}$$

This exchange process was referred previously as the N_{OH^-} process (Nonin *et al.* 1996). It yields to a line of slope −1 in the semilogarithmic plot of the exchange time as a function of pH.

When the acceptor is H_2O (N_{H_2O} process), equation (2) simplifies into:

$$k_{ex,H_2O} = q_{H_2O}\ 10^{-pK_i} \tag{4}$$

This mechanism is pH-independent.

Exchange from the open state depends on the catalyst concentration: (1) under moderate catalyst concentration, the exchange probability per opening event is low. The exchange time is:

$$\tau_{ex} \approx 1/(K_d k_{ex,acc,open}) = \tau_{ex,acc,open}/K_d \tag{5}$$

where K_d is the base-pair dissociation constant. It follows from equation (1)

$$\tau_{ex} \approx \tau_{ex,acc}/\alpha K_d \tag{6}$$

Consequently, when the exchange is mainly governed by the external catalysis process, the apparent dissociation constant, αK_d, is deduced from measurements of the exchange times τ_{ex} of the pair and $\tau_{ex,acc}$ of the corresponding mononucleoside under the same concentration of catalyst.

For example, on a log–log scale, the plots of τ_{ex} and $\tau_{ex,acc}$ as a function of the inverse of the ammonia concentration are straight lines of slope unity, whose relative vertical shift yields αK_d (Leroy *et al.*, 1988b; Guéron *et al.*, 1989; Guéron & Leroy, 1995).

(2) At very high concentration, exchange occurs for each opening event and the opening of the base-pair becomes rate-limiting:

$$\tau_{ex} \approx \tau_0 \qquad (7)$$

where τ_0 is the base-pair lifetime.

Intrinsic catalysis

This exchange process is specific to hydrogen-bonded imino protons within a pair. It occurs through a bridging water molecule to the imino position of the base opposite it in the pair and is efficient as long as this position is not fully protonated. The pK of the acceptor positions involved in Watson–Crick and Hoogsteen base-pairs are below 4.5 at 15°C (pK[N^3C] = 4.34, pK[N^1A] = 3.9, pK[N^7G] = 2.15) (Ts'o, 1974). The rate of the intrinsic catalysis is:

$$k_{ex,int} \approx k_{int}\ 10^{pK_{int}-pK_i} \qquad (8)$$

where k_{int} is a pseudo collision factor that reflects the efficiency of the intrinsic catalysis and depends on the geometry of the open state. The order of magnitude of k_{int} is generally well conserved for the internal Watson–Crick base-pairs of DNA duplexes and ligand–DNA complexes (Guéron, *et al.*, 1987; Nonin, 1995; Nonin *et al.*, 1996). The contribution $k_{ex,int}$ to the exchange rate is pH-independent. The corresponding exchange time τ_{ex} is also called τ_{AAC} (exchange time in the Absence of Added Catalyst) in the literature. As an example, in a Watson–Crick G·C base-pair, the N^3 position of the opposite cytidine (eqn. (8)) has a catalytic efficiency that is about one million times larger than that of water {pK[N^3C] − pK_{H_2O} = [4.3 − (−1.7) = 6]}.

General expression of the imino proton exchange time

For a base-pair of lifetime τ_0 and whose dissociation constant K_d is much less than unity, the experimental imino proton exchange time is:

$$\tau_{ex} \approx \tau_0 + [(1/\Sigma k_{ex,acc,open}) + (1/k_{ex,int})]/K_d \qquad (11)$$

Results

All exchange measurements have been carried out (except as noted) at 15°C, a temperature that yields both convenient exchange times (in the 1 ms to few hundreds of ms range) and well-resolved NMR imino proton spectra of the free 40-mer RNA aptamer and its AMP complex. The imino proton spectra recorded between pH 5.6 and 9.3 did not show any signs of structural transitions or sample degradation over this pH range for either the free RNA aptamer or the AMP complex. The imino protons in the free RNA aptamer and the AMP complex have been assigned in previous structural studies (Jiang *et al.*, 1996b, 1997) and are labeled in this paper by type and position of the individual residues in the 40-mer sequence. The RNA imino proton exchange times are compared with the corresponding exchange times of the rU and rG mononucleosides under comparable conditions of pH and external catalyst concentration. The experimental hydrogen exchange data collected at 400 MHz are fitted according to the theoretical equations outlined in Theory. Our presentation will focus initially on the exchange characteristics of the Watson–Crick stem imino protons, which will provide a reference for the subsequent analysis of the imino protons participating in mismatched pairs and molecular recognition in the ATP-binding asymmetric internal loop of the AMP–RNA aptamer complex.

The stem pairs in the free RNA aptamer

The imino proton resonances of the Watson–Crick base-pairs in the two stems of the free RNA aptamer at pH 7.2 and 15°C are observed between 12.5 and 15 ppm with the previously determined assignments (Jiang *et al.*, 1996b, 1997) listed over the spectrum in Figure 2(a). We do not detect the imino protons of G1 (of the terminal base-pair) and U18 (of the base-pair flanking asymmetric internal loop) while the imino proton of U5 is not resolved (superpositioned with the imino proton of G3) in the spectrum at 15°C.

The U4 imino proton in the free RNA aptamer rapidly broadens out under moderate concentration of added ammonia catalyst as shown in spectra plotted in Figure 2(b). A plot of the exchange time of the imino proton of U4 as a function of pH in the free RNA aptamer (designated U4f) is plotted in Figure 3(b) (open circles). The pH-dependent exchange behavior is similar to what has been commonly observed for Watson–Crick base-pairs in *B*-DNA duplexes. Two processes can be distinguished in this plot: the exchange rate is proportional to OH^- concentration above pH 8.5 and is assigned to the N_{OH^-} process (eqn (3)). The drawn straight line of slope −1 for the U4f resonance in the free RNA is displaced vertically from the corresponding line for the monomer by a factor of 0.5×10^{-4}, which, according to equation (6), gives the value of the apparent dissociation constant (αK_d). Despite this value of the dissociation constant, the exchange around pH 7 is approximately only one order of magnitude slower than the exchange of the monomer imino proton with water measured at pH 5 (N_{H2O} process on the monomer). This, and the fact that exchange of U4f is pH-independent around pH 7, are characteristic

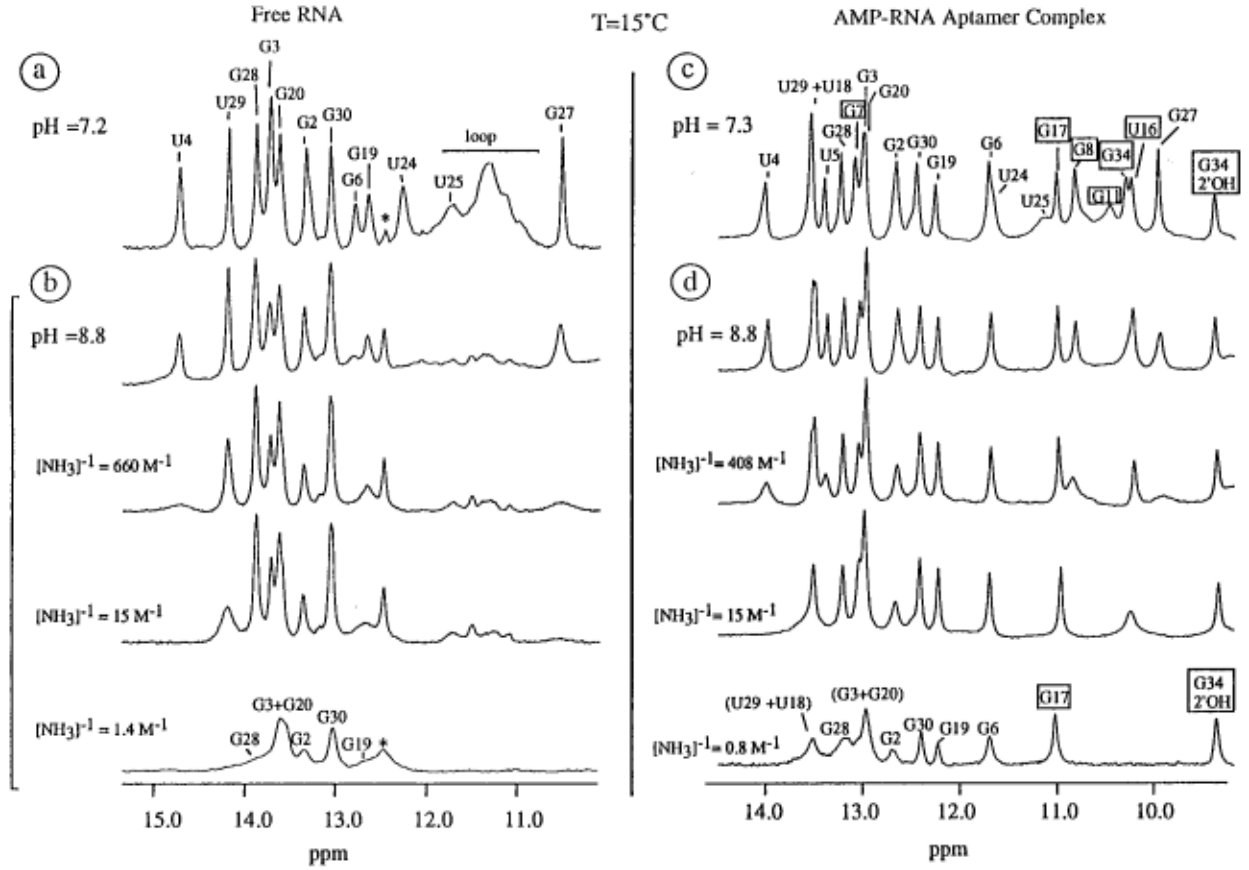

Figure 2. 400 MHz imino proton spectra of the free RNA aptamer and the AMP–RNA aptamer complex in the absence and presence of added ammonia in 2 mM EDTA containing 95% H_2O/5% $^2H_20$ solution at 15°C. (a) Imino proton spectrum of the free RNA aptamer in the absence of ammonia at pH 7.2. The G1 (terminal) and U18 (flanking internal loop) imino protons are too broad while that of U5 is not resolved in the spectrum at this temperature. (b) Imino proton spectra of the free RNA aptamer as a function of increasing concentration of ammonia at pH 8.8. The imino protons of the asymmetric internal binding loop are broadened to the baseline by hydroxide ion catalysis at pH 8.8 (upper spectrum). Hydrogen-bonded imino protons with higher αK_d values (U4, G6) exchange faster in the presence of ammonia than their counterparts with lower αK_d values (G30, U29, G19). Imino protons whose base-pair lifetimes are in the range of few milliseconds (G28, G2 and G19) and whose αK_d values are very low (G30) remain observable at very high concentration of ammonia (lower spectrum). (c) Imino proton spectrum of the AMP–RNA aptamer complex in the absence of ammonia at pH 7.3. All the imino protons in the asymmetric internal binding loop (labeled by squares) are well-resolved in the spectrum. The sugar 2′-OH proton of G34 is observed at 9.4 ppm. The imino protons of U24 and U25 UUCG hairpin loop) and G11 (asymmetric internal loop) are significantly exchange-broadened in this spectrum. (d) Imino proton spectra of the AMP–RNA aptamer complex as a function of increasing concentration of ammonia at pH 8.8. The G11 imino proton of the asymmetric binding internal loop has broadened to baseline by hydroxide catalysis at pH 8.8 (upper spectrum). The imino protons whose base-pair lifetime τ_0 are in the range of a few milliseconds (G28 and G2), and whose αK_d values are low (G6, G19 and G30) remain observable at very high concentrations of ammonia (lower spectrum). The Hoogsteen G17·G34 base-pair is one of the most stable in the complex. The G17 imino proton resonance remains narrow at high concentrations of ammonia (lower spectrum). The linewidth of the sugar 2′-OH proton of G34 is insensitive to ammonia concentration.

of intrinsic catalysis. The effect of added ammonia catalyst on the exchange time of the U4 imino proton in the free RNA is displayed in Figure 3(e). The vertical shift between the line of the monomer and that of the pair yields a αK_d (NH_3) of 4×10^{-4} (Table 1). This value, based on ammonia catalysis, is consistent with the corresponding value derived from hydroxide catalysis.

The pH-dependent exchange times of the remaining resolved stem imino protons in the free RNA aptamer display the same features as the imino proton of U4 (several examples are shown in Figures 3 and 4) and are interpreted in the same manner. The corresponding αK_d (NH_3) values measured from ammonia catalysis are listed in Table 1. The imino proton of G6 like the imino proton of U4 is exchange-broadened under conditions of low OH^- or ammonia concentrations (Figure 2(b)). The apparent dissociation constants of the G3·C38, G20·C31, G30·C21 and G28·C23 base-pairs are too small for their corresponding imino proton exchange values to be significantly

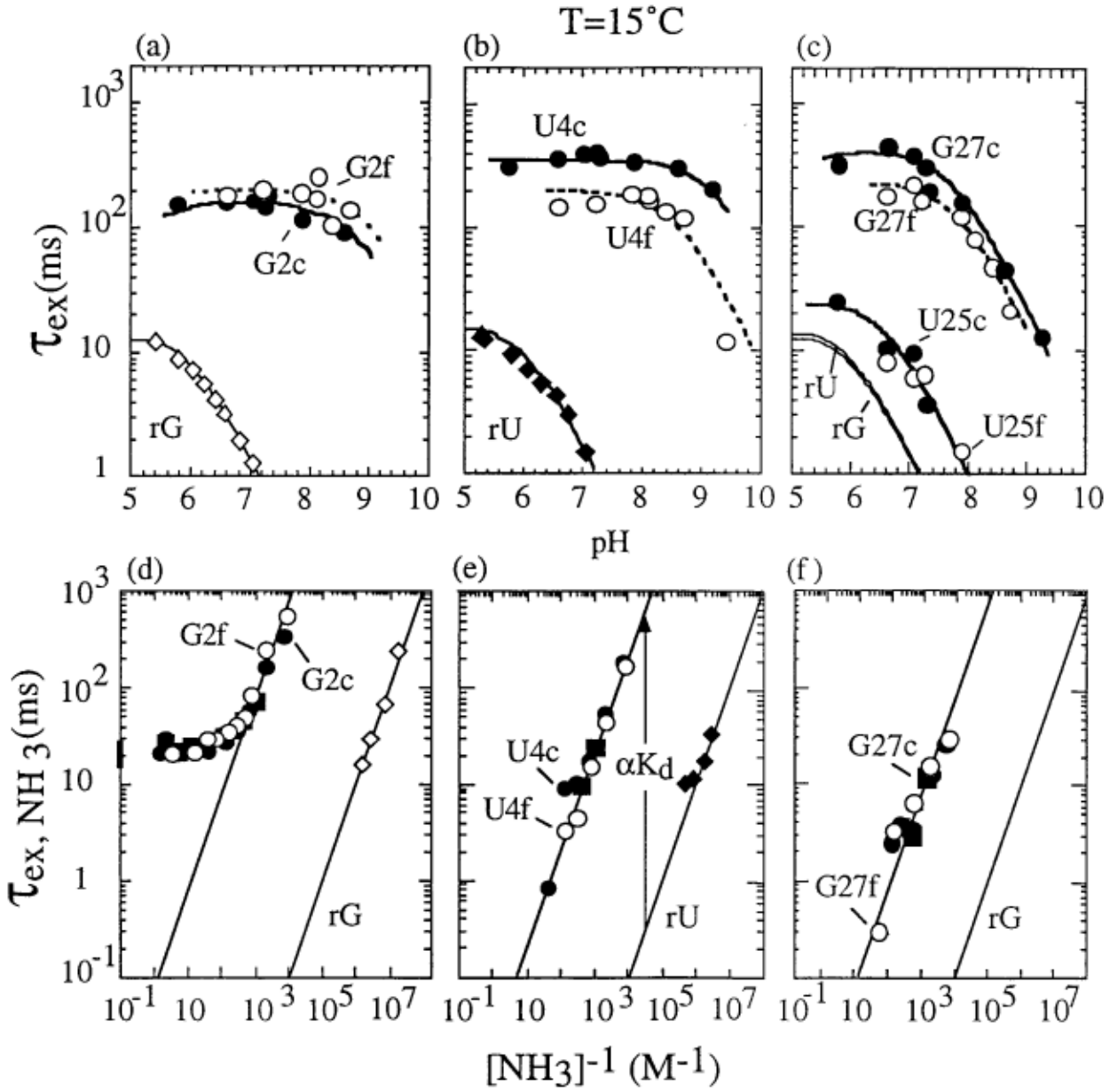

Figure 3. Exchange times of the imino protons in the stem (G2 and U4) and UUCG hairpin loop (G27 and U25) segments in the free RNA aptamer (designated by f) and the AMP–RNA aptamer complex (designated by c) as a function of pH and ammonia at 15°C. The corresponding exchange times in the ribonucleoside monomers under the same conditions are represented by diamonds. The pH dependence of the exchange times of: (a) the G2, (b) the U4 and (c) the G27 and U25 imino protons in the free RNA duplex and the complex. The exchange times are analyzed in term of three exchange processes: the hydroxyl catalysis N_{OH^-} at high pH, the intrinsic catalysis from the neutral hydrogen bond acceptor at the pH-independent plateau and the intrinsic catalysis from the N^7-protonated guanosine for G·C base-pairs under pH 6. The curves are fitted according to equation (11) with the αK_d values listed in Tables 1 and 2, the pK values given in Theory and the following collision and pseudo-collision constants measured on the monomer using equations (3) and (4): for rU, $q_{OH^-} = 6 \times 10^9\ s^{-1}\,M^{-1}$ and $q_{H_2O} = 1.5 \times 10^{11}\ s^{-1}$; for rG, $q_{OH^-} = 6.5 \times 10^9\ s^{-1}\,M^{-1}$ and $q_{H_2O} = 1.65 \times 10^{11}\ s^{-1}$. The lines of the base-pairs are displaced vertically from that of the monomer by a factor whose inverse gives the apparent dissociation constant αK_d (OH^-). The dependence on the inverse of the ammonia concentration of (d) the G2, (e) the U4 and (f) the G27 imino protons in the free RNA duplex and the complex. Filled circles and squares relate to data collected on the complex with one and four equivalents of AMP bound per RNA aptamer, respectively. The same αK_d (NH_3) values are observed for both ratios of AMP in the complex. The lines of the base-pairs are displaced vertically from that of the monomer by a factor whose inverse gives the apparent dissociation constant αK_d (NH_3).

Table 1. Thermodynamic and kinetic parameters of imino proton exchange in the two stems of the free RNA aptamer and its AMP complex at 15°C

Base-pair	free RNA αK_d (NH_3)[a]	AMP–RNA αK_d (NH_3)[a]
G2·C39	7.5×10^{-5}	2.5×10^{-4}
G3·C38[c]	2.5×10^{-5}	(4.3×10^{-6})
U4·A37	4×10^{-4}	4×10^{-4}
U5.A36	–	2.6×10^{-4}
G6·C35	5×10^{-3}	3.6×10^{-7}
U18·A33[b]	–	(5×10^{-6})
G19·C32	3.8×10^{-4}	6.5×10^{-8}
G20·C31[c]	(2.5×10^{-5})	(4.3×10^{-6})
C21·G30	7×10^{-8}	1.5×10^{-7}
A22·U29[b]	6.5×10^{-5}	(8.6×10^{-5})
C23·G28	2.3×10^{-5}	3.2×10^{-5}

[a] Apparent dissociation constants derived from the comparison of the ammonia catalysis acting from the base-pair and from the monomer.

[b] U18 and U29 imino proton resonances are poorly resolved in the complex. The corresponding values are to be taken as an approximation of the real values.

[c] G20 and U5 imino proton resonances are not resolved in the free RNA. G20 and G3 imino proton resonances are poorly resolved in the complex.

effected by OH^- catalysis at pH 9, and their values had to be derived from the experiments using ammonia catalysis. The αK_d values fall roughly in the 10^{-4} to 10^{-7} range for these base-pairs in the free RNA aptamer (Table 1). It should be noted that the exchange times of the G2 and G30 imino protons in the free RNA aptamer are still measurable at high concentrations of ammonia (lowest spectrum in Figure 2(b)). The base-pair lifetimes, τ_0, for the G28·C19 and G2·C39 pairs are in the range 10 to 15 ms and around 20 ms, respectively. A very high ammonia concentration would be required to estimate the base-pair lifetime for the G30·C19 pair because of its very low apparent dissociation constant ($\alpha K_d = 7\ 10^{-8}$) in the free RNA aptamer.

The UUCG hairpin loop in the free RNA aptamer

The imino protons of U24, U25 and G27 of the stable UUCG hairpin loop are observed as resolved resonances in the NMR spectrum of the free RNA aptamer at 15°C in Figure 2(a). The plot of the pH dependence of the exchange times for the G27 imino proton in the UUCG hairpin loop (Figure 3(c), open circles) in the free RNA aptamer is similar to that observed for imino protons in the stem segment. The hydroxide and ammonia catalysis of exchange are, respectively, 10^3 and 7.7×10^5 times less efficient than the corresponding values for the monomer (Figures 3(c) and (f)). The exchange of G27 is governed by intrinsic catalysis around pH 6.5 and is only 17 times slower than the monomer at pH 5.

The U24 and U25 imino proton resonances of the UUCG hairpin loop are exchange broadened to baseline in the pH 8.8 spectrum of the free RNA aptamer (Figure 2(b), top spectrum). Their N_{OH^-} straight lines are shifted by a factor of 1.2×10^2 (data not shown) and 5.9 (Figure 3(c)), respectively. However, the slowest exchange times measured for both these protons (U24 around pH 7) and (U25 around pH 6) are close to those measured for the uracil monomer N_{H_2O} process.

The asymmetric internal loop in the free RNA aptamer

The imino protons of the asymmetric internal loop are observed as broad resonances centered about 11.3 ppm in the free RNA aptamer spectrum (Figure 2(a), upper spectrum). This precludes any attempts to measure the exchange behavior of the imino protons of the ATP-binding asymmetric internal loop in the free RNA aptamer.

Characteristics of the AMP–RNA aptamer complex

The 400 MHz exchangeable proton NMR spectrum of the AMP–RNA aptamer complex (one equivalent of bound ligand) in water (pH 7.3 at 15°C) exhibits well-resolved imino, amino and sugar 2′-hydroxyl resonances with the previously determined assignments (Jiang *et al*. 1996b,c) listed over the spectrum in Figure 2(c). These assignments include those for the imino protons in the critical ATP-binding asymmetric internal loop of the complex, which are boxed in Figure 2(c). The exchange times of the resolved imino protons in the complex have been followed as a function of basic pH and added ammonia using approaches similar to those described above for the free RNA aptamer. Some of these measurements were also undertaken for complexes containing excess AMP (four equivalents) in order to shift the equilibrium between the free RNA and the complex toward the latter species. We measure identical ammonia contributions to the exchange times ($\tau_{ex,NH_3}/\alpha K_d$) for even the strongest base-pairs, for data collected on the complexes containing stoichiometric (one equivalent) or excess (four equivalents) of AMP. We conclude that the dissociation of the complex does not contribute to the exchange process and that imino proton exchange in the AMP–RNA aptamer complex can be interpreted in terms of base-pair opening and not of complex dissociation.

The stem pairs in the AMP–RNA aptamer complex

The apparent dissociation constants for the imino protons of the stem base-pairs in the AMP–RNA aptamer complex were measured using proceedures described above for the free RNA aptamer and are listed in Table 1. The imino proton of U4 is well resolved in the specrtum of the complex in Figure 2(c) and broadens on addition of moderate concentrations of ammonia as shown in Figure 2(d). The plot of its exchange time as a function of pH (filled circles, Figure 3(b)) shows that its

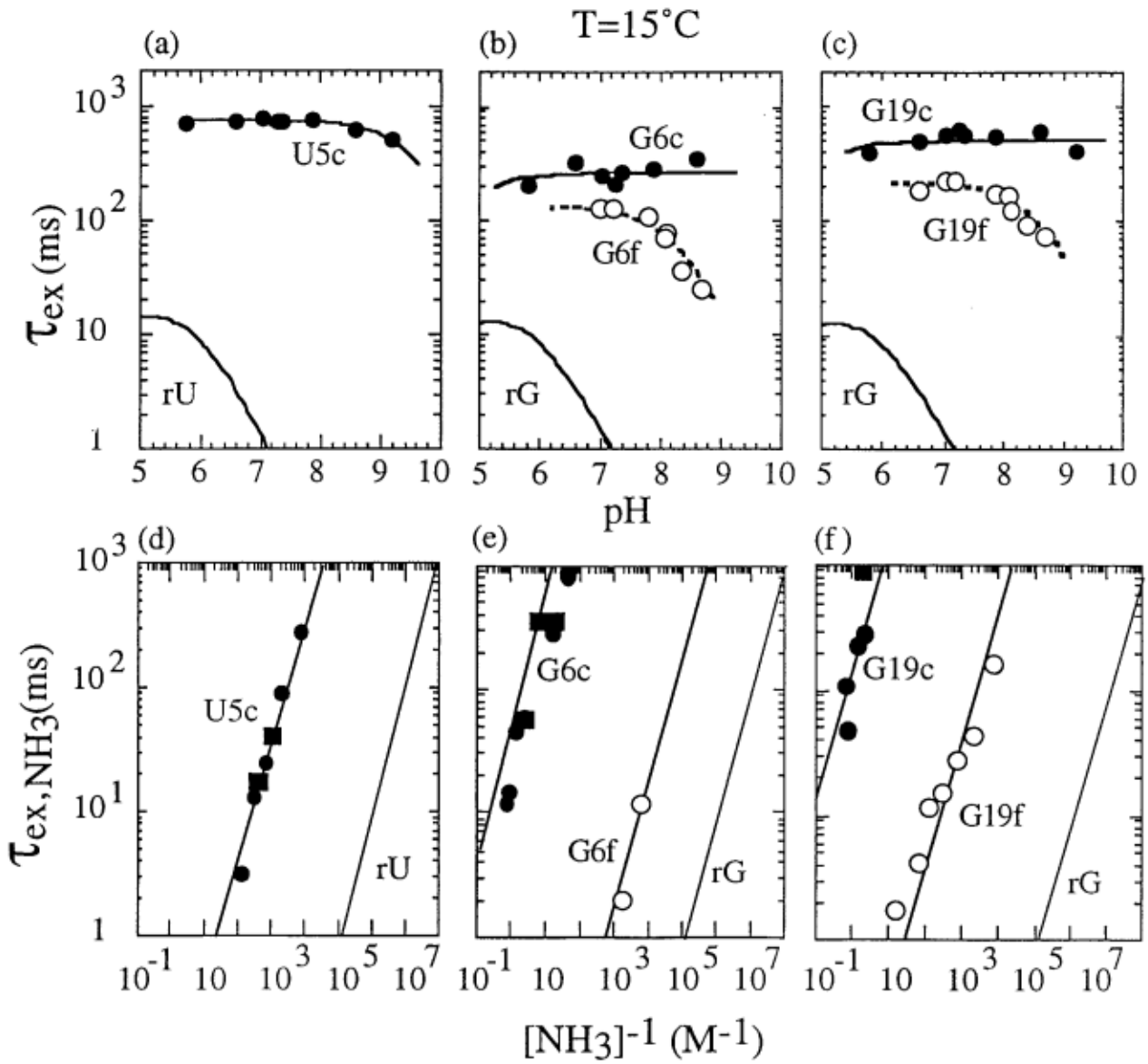

Figure 4. Exchange times of imino protons of three base-pairs flanking either side of the ATP-binding asymmetric internal loop in the free RNA aptamer (designated by f) and the AMP–RNA aptamer complex (designated by c) as a function of pH and ammonia at 15°C. The corresponding curves describing exchange times in the ribonucleoside monomers under the same conditions are included in the plots. The pH dependence of the exchange times of: (a) the U5, (b) the G6 and (c) the G19 imino protons in the free RNA duplex and the complex. The dependence on the inverse of the ammonia concentration of: (d) the U5, (e) the G6 and (f) the G19 imino protons in the free RNA duplex and the complex. Filled circles and squares relate to data collected on the complex with one and four equivalents of AMP bound per RNA aptamer, respectively. The same αK_d (NH_3) values are observed for both ratios of AMP in the complex.

catalysis by hydroxide ion is about three times less efficient than it is in the free RNA (open circles, Figure 3(b)). The apparent dissociation constant measured from ammonia catalysis of the U4·A37 pair is the same in the free RNA aptamer and its AMP complex (Figure 3(e)).

The imino protons of the superpositioned U29 and U18, superpositioned G3 and G20 and resolved G28, G2, G30, G19 and G6 residues are still observable even under drastic conditions of added ammonia catalyst as shown in Figure 2(d) (lowest spectrum). The ammonia exchange time contribution for the imino protons of G2 and G28 extrapolate at infinite concentration of ammonia (a measure of base-pair lifetime, τ_0) to 20 ms (Figure 3(d)) and between 6 and 10 ms (data not shown), respectively.

The UUCG hairpin loop in the AMP–RNA aptamer complex

The exchange characteristics of the U25 and G27 imino protons of the UUCG hairpin loop have been monitored in the AMP–RNA aptamer com-

plex (data points labeled U25c and G27c in Figure 3(c) and (f)) with the measured apparent dissociation constant values listed in Table 2. We observe similar hydroxide and ammonia catalysis for these UUCG hairpin loop imino protons in the free RNA aptamer and its AMP complex.

The asymmetric internal loop in the AMP–RNA aptamer complex

We observe six well-resolved asymmetric internal loop imino protons from the G7, G8, G11, U16, G17 and G34 residues in the AMP–RNA aptamer complex at pH 7.3 and 15°C (Figure 2(c)). All these imino protons except for G11 exchange in a few hundreds of ms independently of pH between 6.5 and 7.0, as shown in the upper panels of Figure 5. These exchange times of the asymmetric internal loop imino protons in the complex are about an order of magnitude slower than their counterparts in the free monomer. The reduction of the efficiency of hydroxide ion catalysis for these imino protons in the complex relative to the monomer range from two orders of magnitude (G11), to three orders of magnitude (G34), to greater than four orders of magnitude (G7, G8, U16 and G17) as shown in the upper panels of Figure 5. The apparent dissociation constants for G7, G8, U16, G17 and G34 in the complex were estimated from their exchange characteristics as a function of added ammonia (lower panels of Figure 5) and are listed in Table 2.

The G11 imino proton in the complex exchanges in the 40 ms range at pH 6.6 and 15°C, which is close to the value of 14 ms observed for the guanosine monomer control under the same conditions (Figure 5(a)). The G11 imino proton rapidly broadens out above pH 8 and at low concentration of ammonia (Figure 2(d)). The N_{OH^-} process for the G11 imino proton in the complex is 0.5×10^{-2} less efficient than for the corresponding the monomer. The exchange times measured around pH 6.6 are thus 18 times shorter than what is expected from the uncatalyzed exchange with water.

Table 2. Thermodynamic and kinetics parameters of imino proton exchange in the asymmetric internal binding and UUCG loops of the free RNA aptamer and its AMP complex at 15°C

Imino proton	free RNA αK_d (NH_3)[a]	AMP–RNA αK_d (NH_3)[a]
U24	8.5×10^{-3}[b]	
U25	0.17[b]	0.17[b]
G27·U24	1.6×10^{-3}	1.6×10^{-3}
G7·G11	–	1.45×10^{-5}
G8[c]	–	3.1×10^{-4}
G11[c]	–	2×10^{-2}[b]
U16[c]	–	7.5×10^{-6}
G17·G34	–	4.3×10^{-7}
G34[c]	–	1.6×10^{-2}

[a] Apparent dissociation constants derived from the comparison of the ammonia catalysis acting from the base-pair and from the monomer.

[b] Apparent dissociation constants derived from the comparison of the N_{OH^-} process acting from the base-pair and from the monomer.

[c] These imino protons whose hydrogen bond status was not discussed in the previously published solution structure (Jiang *et al.*, 1996a) are clearly hydrogen-bonded based on the imino proton exchange and base-pair kinetics studies outlined in the experiemental data in the current study (Figure 5).

The sugar 2′-OH proton of G34 in the complex

The sugar 2′-OH proton of G34 resonates downfield at 9.4 ppm in the exchangeable proton spectrum of the complex at 15°C and remains narrow in the pH 5 to 8 range (Figure 2(c) and (d)). It exhibits a longitudinal relaxation time (T_1) of 119 ms at pH 8.7 for complexes containing either stoichiometric (one equivalent) or excess (four equivalents) of AMP. Its T_1 value decreases slightly to 96 ms on increasing the ammonia concentration to $1/[NH_3] = 2\,M^{-1}$ (Figure 6(a)). In order to access the exchange times of the sugar 2′-OH proton of G34 in the complex, we measured T_1 values with and without added ammonia in the complex (containing four equivalents of AMP) at pH 8.7 between 0°C and 45°C. The T_1 values are independent of added ammonia concentration over this temperature range (Figure 6(b)) but are dependent on temperature with dipolar contributions predominating below 25°C and exchange contributions predominating above 30°C. The T_1 values are a measure of τ_{ex} in the high temperature range and extrapolation of this exchange data yields an exchange time in the range of ten seconds for the sugar 2′-OH proton of G34 in the complex at 15°C. The same exchange time value can also be computed from the experimental T_1 data assuming a dipolar contribution of 120 ms between 15°C and 25°C.

Discussion

Exchange processes reflect base-pair opening

An increase of the AMP concentration should shift the free RNA/complex equilibrium towards the formation of the complex. All imino protons must exchange from the open base-pairs in the complex, since no changes are observed in the apparent dissociation constants of complexes containing either one or four equivalents of AMP (lower panels of Figures 3 to 5).

Distinction between free and hydrogen bonded imino protons

The theory of imino proton exchange (see Theory) allows one to distinguish between imino protons that are hydrogen-bonded and those that are protected from external catalysts. Imino protons from the former class all share the same feature: their exchange times are somewhere pH-independent, and the exchange time τ_{AAC}

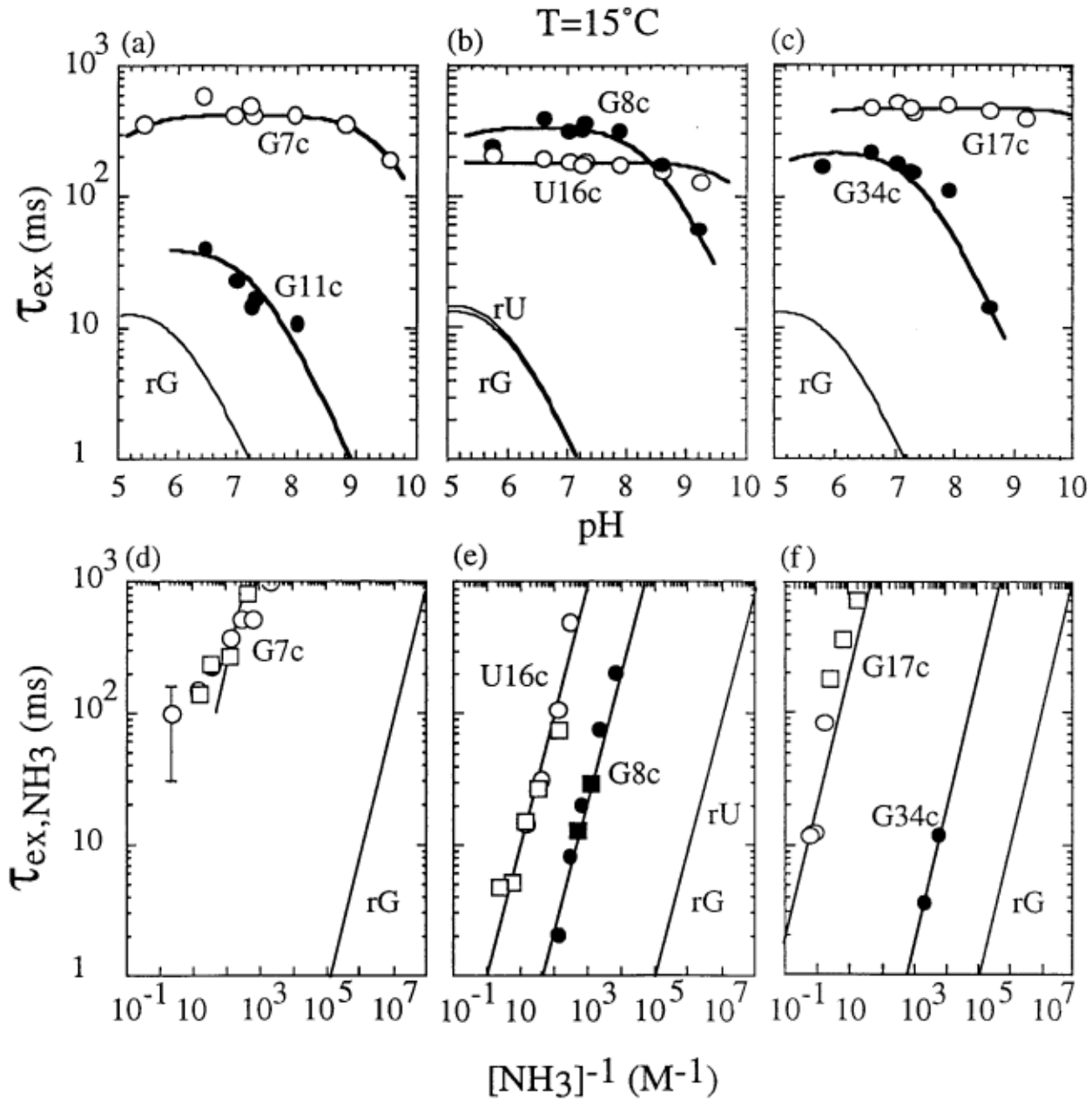

Figure 5. Exchange times of imino protons in the ATP-binding asymmetric internal loop in the AMP–RNA aptamer complex as a function of pH and ammonia at 15°C. The corresponding curves describing exchange times in the ribonucleoside monomers under the same conditions are reported in the plots. The pH dependence of the exchange times of: (a) the G7 and G11 imino protons, (b) the G8 and U16 imino protons and (c) the G17 and G34 imino protons in the complex. Exchange times of all imino protons except G11 (for which the data are marginal to reach conclusions) display the pH-independent feature characteristic of intrinsic catalysis. The apparent dissociation constants of base-pairs involving the imino protons of G7, U16 and G17 are too low to be derived from the hydroxide catalysis data. The dependence on the inverse of the ammonia concentration of: (d) the G7 imino proton, (e) the G8 and U16 imino protons and (f) the G17 and G34 imino protons in the complex. Circles and squares relate to data collected with one and four equivalents of AMP bound per RNA aptamer, respectively. The same αK_d (NH_3) values are observed for both ratios of AMP in the complex.

measured at the plateau is shorter than what is expected from the apparent dissociation constant and the exchange with water from the monomer. The accelaration is due to the p*K* difference between water (−1.7) and the intrinsic acceptor (around 4 in Watson–Crick base-pairs). For comparison, a ''free'' imino proton sterically protected from exchange with solvent could display a reduction in the efficiency of external catalysis by a factor comparable to what is observed due to the apparent dissociation constant, but such a factor would be expected over the entire pH range. No acceleration, and no pH-independent plateau are observed.

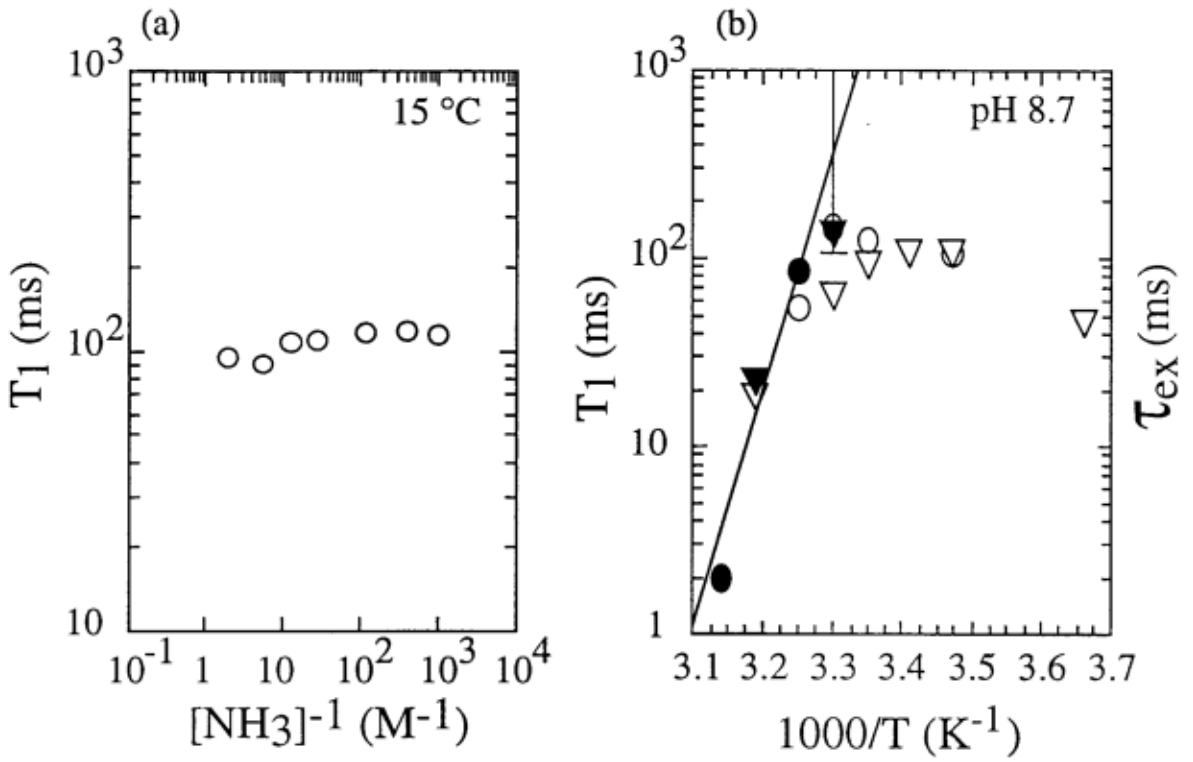

Figure 6. (a). The longitudinal relaxation time T_1 of the sugar 2′-OH proton of G34 as a function of the inverse of ammonia concentration in the AMP–RNA aptamer complex at 15°C. The T_1 values are independent of the ammonia concentration upto 0.5 M. (b) The longitudinal relaxation times T_1 (open symbols) and exchange times (filled symbols) of the sugar 2′-OH proton of G34 as a function of temperature at pH 8.7 in the absence (triangles) and in the presence (circles) of 12 mM ammonia. The relaxation is governed by dipolar processes around 15°C and by chemical exchange contributions at higher temperatures. At high temperature T_1 is equal to τ_{ex}. An extrapolation of the exchange times measured at high temperature yields a τ_{ex} of about 20 seconds at 15°C and one second at 25°C. The same result is obtained, based on the computation of τ_{ex} from T_1 assuming a dipolar contribution of 120 ms between 15 and 20°C.

The stem imino protons

These imino protons are Watson–Crick base-paired and their exchange properties do not differ from what is currently observed in *B*-DNA duplexes. The apparent dissociation constants, αK_d (NH_3), measured from ammonia catalysis are listed in Table 1 and exhibit similar values for the G2·C39, G3·C38, U4·A37, G20·C31, C21·G30, A22·U29 and C23·G28 base-pairs in the free RNA aptamer and its AMP complex (Figure 7). The apparent dissociation constants span the 10^{-4} to 10^{-6} range except for the C21·G30 and G19·C32 base-pairs whose αK_d (NH_3) values are in the 10^{-7} to 10^{-8} range in the complex (Figure 7).

The UUCG loop imino protons

The UUCG hairpin loop is a common stable secondary structural fold in RNA. A revised NMR-based solution structure has recently been reported that has defined the conformation of this hairpin loop (Allain & Varani, 1995). The exchange characteristics of the imino proton of G27 (9.90 ppm) as a function of hydroxide ion and ammonia catalysis are plotted in Figure 3(c) and (f) respectively, for both the free RNA aptamer and the AMP–RNA aptamer complex. The pH-independent exchange times are in the range 200 to 400 ms in the pH range 5.5 to 7.0 (Figure 3(c)) and similar αK_d (NH_3) values of 1.6×10^{-3} are observed for both the free RNA aptamer and the AMP–RNA aptamer complex (Figure 3(f) and Table 2). These patterns require that the imino proton of G27 participate in a hydrogen bond in the UUCG hairpin loop of both the RNA aptamer and the AMP–RNA aptamer complex. This is consistent with the solution structure of the UUCG hairpin loop reported previously (Allain & Varani, 1995) and, based on this structure, the imino proton of G27 is most likely hydrogen-bonded to one of the carbonyl oxygen atoms of U24 in the free RNA aptamer and in the complex.

The imino proton of U25 (11.29 ppm) is strongly sensitive to exchange catalysis in both the free RNA aptamer (Figure 2(a)) and the AMP–RNA aptamer complex (Figure 2(b)). Its exchange characteristics as a function of pH approach that of ribouridine (Figure 3(c)) implying that it is not base-paired in either the free RNA aptamer or the complex. The imino proton of U25 is the most solvent-exposed imino proton in the AMP–RNA aptamer complex (Table 2).

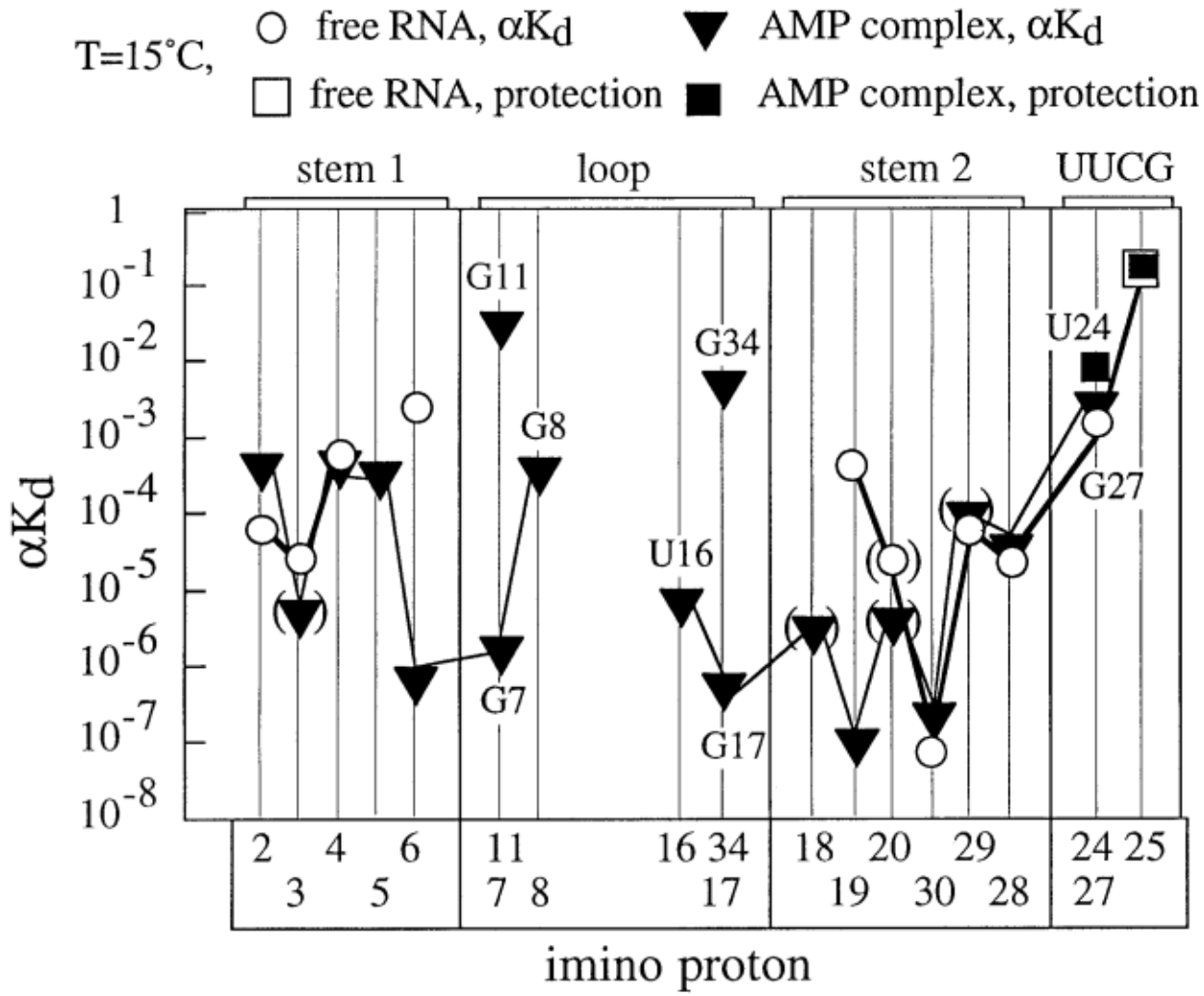

Figure 7. Plot of the apparent dissociation constants (circles and triangles) and the protection factors (squares) as a function of the base-pair or base position in the free RNA aptamer (open symbols) and in the AMP–RNA aptamer complex (filled symbols). The bracketed symbols correspond to αK_d values derived from the measurement of exchange times from poorly resolved imino proton resonances and must be considered the best estimate at this time. Apparent dissociation constants of the Watson–Crick base-pairs of the two stems do not differ from the values commonly observed in B-DNA. Complexation with AMP enhances the stability of the base-pairs flanking the ATP-binding asymmetric internal loop. This effect is negligible beyond the second base-pair. The apparent dissociation constants of the base-pair mismatches fall in the same range as that of the stem Watson–Crick base-pairs. These values for G·G mismatches involving G7 and G17 imino protons are among the most stable in the complex. The protection from hydroxide catalysis estimated for the imino protons of G11 and U24 are of comparable magnitude.

Base-pairs flanking the ATP-binding asymmetric internal loop

The αK_d (NH_3) values for the G6·C35 (Figure 4(e)) and G19·C32 (Figure 4(f)) base-pairs measured from ammonia catalysis are lowered by about four orders of magnitude on complex formation. Interestingly, the αK_d (NH_3) value of 6.5×10^{-8} for the G19·C32 base-pair identifies it as the most stable pair of the AMP–RNA aptamer complex.

The U5 imino proton peak is not resolved in the spectrum of the free RNA at 15°C (Figure 2(a)) but it is resolved in the spectrum of the complex (Figure 2(c)). The αK_d (NH_3) value of the U5·A36 base-pair is 2.6×10^{-4}. The imino proton of the U5 resonance is resolved at 0°C in the free RNA and its line width is a little larger than in the complex, suggesting that the U5·A36 base-pair is stabilized in the complex.

The U18 imino proton, which is next to the asymmetric internal loop binding loop, cannot be observed in the spectrum of the free RNA (Figure 2(a)), suggesting that it is not base-paired in the absence of bound ligand. The U18 imino proton is overlapped with the U29 imino proton in the 400 MHz spectrum (but not the 600 MHz spectrum) of the complex (Figure 2(b)). Analysis of the experimental data and the comparision of the evolution of the peak intensity *versus* $[NH_3]^{-1}$ with that of better resolved signals (for example, G7c and U16c) suggests that its αK_d (NH_3) spans the range

10^{-5} to 10^{-6} which would correspond to a million-fold stabilization on complex formation.

The effect of complexation on the stem base-pair apparent dissociation constants

The above results establish that the αK_d (NH_3) values for the base-pairs flanking the ATP-binding asymmetric internal loop in the RNA aptamer are most sensitive to complexation by the bound AMP (Table 1). This is clearly the case for the G6·C35 (flanking position) and G19·C32 (next nearest neighbor flanking position) base-pairs (Figure 7) whose αK_d (NH_3) values are about ten thousand times smaller than the corresponding apparent dissociation constants in the free RNA aptamer. By comparision, αK_d (NH_3) values for the G2·C37, U4·A37 and G27·U24 pairs are identical in the free RNA and in the complex (Figure 3, lower panels). Our imino proton exchange and base-pair kinetics studies establish that the extent of stabilization on complex formation appears to be maximal for the base-pairs that directly flank the asymmetric internal loop and that the stabilization of the stem extends to the second neighbor base-pairs on either side of the ATP-binding asymmetric internal loop on complex formation.

The imino protons of the ATP-binding asymmetric internal loop in the complex

The solution structure of the AMP–RNA aptamer complex established that the ATP-binding asymmetric internal loop contains mismatched pairs that are key to the organization of the RNA fold and recognition of the bound AMP ligand (Jiang *et al.*, 1996a,b; Dieckmann *et al.*, 1996). We have applied the imino proton exchange theory developed for Watson–Crick base-pairs in duplex DNA to interpret the kinetics of mismatched pairs within the ATP-binding asymmetric internal loop of the AMP–RNA aptamer complex.

The plots of exchange times as a function of pH for the imino protons of G7, G8, U16, G17 and G34 in the complex display a pH-independent plateau within which the exchange of all these asymmetric internal loop imino protons are governed by the intrinsic catalysis (Figures 5(a), (b) and (c)). This leads to the conclusion that these five imino protons are hydrogen bonded in the complex, independently of any assumption of the structure. Consequently, the vertical shifts observed in the slopes associated with catalysis by an external acceptor (OH^- or NH_3) can be interpreted in terms of the apparent dissociation constant for the interaction (occurring either between two bases or between a base and a non-base acceptor). The catalysis by hydroxide ions is observed at pH 9 for the imino protons of G8 (Figure 5(b)) and G34 (Figure 5(c)), and to a lesser extent for the imino proton of G7 at pH 9.5 (Figure 5(a)) in the complex. The pH-independent plateau extends to pH 9 for the imino protons of U16 (Figure 5(b)) and G17 (Figure 5(c)), and only an upper limit of the apparent dissociation constants can be derived from the catalysis by hydroxide ions for the mismatched pairs involving the G7, U16 and G17 imino protons in the complex. The corresponding αK_d (NH_3) values (Table 2) estimated from measurements involving ammonia catalysis (Figure 5(d), (e) and (f)) establish that the corresponding mismatch alignments involving these imino protons in the complex are as stable as regular Watson–Crick base-pairs.

The G7·G11 mismatch pair in the complex

A chain reversal occurs within the G7 to G11 segment involving formation of a GNRA loop (the AMP replaces the A in the GNRA loop) closed by a reversed Hoogsteen G7·G11 mismatch pair (Figure 1(b)) in the solution strucuture of the AMP–RNA aptamer complex (Jiang *et al.*, 1996a; Dieckmann *et al.*, 1996). We measure an αK_d (NH_3) value of 1.45×10^{-5} (Figure 5(d) and Table 2) and a pH independent τ_{AAC} of 400 ms between pH 5.5 and 9.0 (Figure 5(a)) for the imino proton of G7 (13.24 ppm) which is hydrogen-bonded to the N^7 acceptor of G11 in the G7·G11 mismatch pair (Figure 1(b)) in the complex. The magnitude of these αK_d and τ_{AAC} values are comparable to what is commonly measured for an internal Watson–Crick base-pair in a *B*-DNA duplex. The pseudo collision factor ($k_{int} = 2.6 \times 10^{12}$) computed from the measurement of τ_{AAC} and αK_d according to equations (8) and (11) indicates efficient intrinsic catalysis of the exchange process.

We observe an αK_d of 2×10^{-2} measured from hydroxide catalysis for the association involving the imino proton of G11 (Figure 5(a) and Table 2) in the complex. The imino proton of G11 (10.41 ppm) can form a weak hydrogen bond with the sugar O-4′ oxygen of C35 in the refined solution structures of the complex (imino proton to oxygen distances range between 2.80 and 3.23 Å) (Jiang *et al.*, 1996a). This weak hydrogen bond, which would be in the mean plane of the C35 sugar and perpendicular to the plane of the G7·G11 base-pair, could account for the exchange characteristics of the G11 imino proton in the complex.

The G17·G34 mismatch pair in the complex

The G17 and G34 bases on opposite sides of the asymmetric internal loop form a Hoogsteen G17(*anti*)·G34(*syn*) mismatch pair (Figure 1(c)) in the AMP–RNA aptamer complex (Jiang *et al.*, 1996a; Dieckmann *et al.*, 1996). The imino proton of G17 (11.06 ppm) is hydrogen bonded to the O^6 acceptor of G34 within the G17·G34 mismatch (Figure 1(c)) and stacks on the G18·C33 pair of the rightward helical stem in the complex. The low αK_d (NH_3) of 4.3×10^{-7} (Figure 5(f) and Table 2) monitored by the G17 imino proton of the G17·G34 mismatch readily explains why the G17

imino proton in the complex remains observable at very high concentrations of ammonia (lowest spectrum in Figure 2(d)).

The existence of a pH-independent intrinsic catalysis ($\tau_{AAC} = 200$ ms, Figure 5(c)) requires the imino proton of G34 to be hydrogen bonded to an acceptor in the complex. The ammonia catalysis of the imino proton of G34 exhibits an αK_d (NH_3) value of 1.6×10^{-2} (Figure 5(f) and Table 2) for the association of G34 with the acceptor in the complex. The imino proton of G34 (10.33 ppm) can form a hydrogen bond to the A14 O^2P of the A13–A14 step in the refined structures of the complex (imino proton to oxygen distances range between 1.80 and 2.69 Å) (Jiang *et al.*, 1996a).

The G8 imino proton in the complex

A pair of hydrogen bonds between the Watson–Crick edge of AMP and the minor groove edge of G8 (Figure 1(d)) defines the key sequence-specific molecular recognition element in the AMP–RNA aptamer complex (Jiang *et al.*, 1996a; Dieckmann *et al.*, 1996). The existance of a pH-independent intrinsic catalysis ($\tau_{AAC} = 350$ ms, Figure 5(b)) requires the imino proton of G8 to be hydrogen-bonded to an acceptor in the complex. The ammonia catalysis of the imino proton of G8 exhibits an αK_d (NH_3) value of 3.1×10^{-4} (Figure 5(e) and Table 2) for the association of G8 with the acceptor in the complex. The G8 imino proton (10.72 ppm) can form a hydrogen bond to the G11 O^1P of the A10–G11 step in the refined structures in the complex (imino proton to oxygen distances range between 1.58 and 2.61 Å) (Jiang *et al.*, 1996a).

The U16 imino proton in the complex

The U16 residue is part of a stacked element spanning the A13 to G17 segment within the asymmetric internal loop in the solution structure of the AMP–RNA aptamer complex (Jiang *et al.*, 1996a; Dieckmann *et al.*, 1996). The exchange time measurements on the U16 imino proton as a function of pH (τ_{AAC} of 200 ms between pH 5.5 and 9, Figure 5(b)) and catalyzed by ammonia (Figure 5(e)), establish the presence of a hydrogen bond involving this imino proton with an αK_d (NH_3) of 7.5×10^{-6}. The U16 imino proton (10.2 ppm) can form a weak hydrogen bond to the N^1 of A12 in the refined structures in the complex (imino proton to nitrogen distances range between 3.28 and 4.09 Å) (Jiang *et al.*, 1996a). Such a U16·A12 pairing stabilized by a potential single weak hydrogen bond (differs from a Watson–Crick U·A pair, since the base planes of U and A are far from coplanar) would be consistent with the NOE observed between the imino proton of U16 and the H2 proton of A12 in the AMP–RNA aptamer complex.

Apparent dissociation constants of base-pair mismatches

The Hoogsteen G17·G34, the reverse Hoogsteen G7·G11 and the U16·A12 pairs of the ATP-binding asymmetric internal loop are as stable as the internal base-pairs of the helical stems in the AMP–RNA aptamer complex (Figure 7). The apparent dissociation constants for the two examples (involving G8 and G34) where hydrogen bonds are formed between the imino protons and the phosphate oxygen atoms as acceptors are in the range of the αK_d (NH_3) values reported for the second terminal Watson–Crick base-pairs measured in *B*-DNA helices (Nonin *et al.*, 1995). The protection of the G11 and U25 imino protons from hydroxide ion catalysis is similar.

The sugar 2′-OH proton of G34

A detailed understanding of the exchange mechanisms of the narrow 9.4 ppm sugar 2′-OH proton of G34 in the AMP–RNA aptamer complex is beyond the scope of the present investigation. Nevertheless, it is possible to draw some conclusions from the experimental data on hand and these are outlined below. The relaxation of this exchangeable proton is mainly driven by dipolar processes except at high temperatures (Figure 6(b)). The chemical exchange contribution to the relaxation process of this proton becomes more efficient than the dipolar contribution with increasing temperature. An extrapolation of the exchange times measured at high temperature yields an exchange time τ_{ex} of about 20 seconds at 15°C (Figure 6(b)). By contrast, the corresponding sugar 2′-OH proton of a ribonucleoside monomer is exchange broadened to baseline reflecting a τ_{ex} far smaller than 1 ms under the same conditions of temperature and external catalyst concentration. The demonstration that the exchange time from the sugar 2′-OH proton of G34 is significantly longer than its monomer counterpart strongly supports its participation in hydrogen bond formation. Indeed, the sugar 2′-OH proton of G34 is both buried and hydrogen-bonded to the N^7 of A12 in the solution structure of the AMP–RNA aptamer complex (Jiang *et al.*, 1996a).

We have observed identical exchange times for the sugar 2′-OH proton in the AMP–RNA aptamer complex derived from the extrapolation of T_1 values both in the absence and presence of NH_3 (80 mM) catalysis. The lack of efficiency of the ammonia catalysis may be explained either by a very low apparent dissociation constant, and/or by the existence of a more efficient mechanism of exchange (intrinsic catalysis by the hydrogen bond acceptor N^7 position of A12) in the complex.

Implications for additional hydrogen bonding alignments

The proton exchange and base-pair kinetics parameters determined for the imino protons of

the ATP-binding asymmetric internal loop in the complex are consistent with the previously published solution structure of the AMP–RNA aptamer complex (Jiang *et al.*, 1996a; Dieckmann *et al.*, 1996). In addition, the present kinetics studies require the formation of hydrogen bonds involving the imino protons of G8, G11, U16 and G34 within the binding pocket that could participate in the stabilization of the complex. The hydrogen-bonding potential of these imino protons was not discussed in the structural paper but a measurement of hydrogen-bonding distances shows that G8, G11, U16 and G34 imino protons can form potential hydrogen bonds with acceptor atoms in the refined solution structures of the complex published by Jiang *et al.* (1996a). Some of these hydrogen bonds are on the long side in the previously refined structures of the complex but could adopt standard lengths following minor conformational adjustments in the structures following further refinement. Future molecular dynamics computations can address this issue by exploring the trends in the measured root-mean-square deviations of the refined structures of the AMP–RNA aptamer complex following incorporation of these hydrogen bonds as loose restraints to guide the calculations.

Materials and Methods

Oligomer preparation and NMR samples

The NMR samples of the AMP–RNA aptamer complex used for the imino proton exchange and base-pair kinetics were the same as used for the NMR data collection that resulted in solving the solution structure of the complex (Jiang *et al.*, 1996a,b). The samples were dialyzed twice against 20 mM NaCl 1 mM EDTA-containing water solutions followed by several dialyses against 1 mM EDTA-containing water to remove potential basic contaminants prior to their use for collection of kinetic data. No noticeable loss of bound AMP was observed after extensive dialysis of the complex. The free RNA aptamer and the AMP–RNA aptamer complex were lyophilized and subsequently dissolved in 2 mM EDTA containing 95% H_2O/5% ^2H_2O phosphate-free solutions. The pH was measured at room temperature using a calibrated PMH82 Radiometer pH-meter and pH values adjusted under vortexing using 0.01 to 0.1 M NaOH and HCl solutions. The stoichiometry of the AMP–RNA aptamer complex was monitored by recording the proton NMR spectrum. Two samples of the AMP–RNA complex were prepared containing one and four equivalents of added AMP per RNA aptamer molecule. Ammonia was added under stirring from stock solutions ranging from 0.01 M to 6 M at pH 8.8. Ammonia-free samples of the RNA aptamer and the AMP–RNA aptamer complex could be recovered after dialysis.

NMR spectroscopy

NMR experiments were acquired on a Varian Unity plus 400 MHz spectrometer with the data processed using the Varian VNMR program. We chose not to collect data at higher field strengths (500 and 600 Mhz) to reduce problems related to radiation damping during the saturation transfer experiments. NMR experiments leading to the determination of imino proton exchange times, apparent dissociation constants and base-pair lifetimes were carried out as described (Leroy *et al.*, 1988b; Guéron *et al.*, 1989; Guéron & Leroy, 1995). They rely on saturation transfer from water (Forsèn & Hoffman, 1963), inversion recovery experiments using a DANTE sequence for saturation or inversion (Morris & Freeman, 1978; Leroy *et al.*, 1988b) and the jump-and-return sequence for water suppression (Plateau & Guéron, 1982). The free induction decays (FIDs) were multiplied by an exponential function leading to a 3 Hz broadening prior to Fourier transformation. The residual water signal was post-acquisitionaly suppressed using the VNMR software routine.

Acknowledgements

We thank Dr J. L. Leroy for stimulating discussions. This work was supported by NIH GM 54777 to D.J.P.

References

Allain, F. H.-T. & Varani, G. (1995). Structure of the P1 helix from group I self-splicing introns. *J. Mol. Biol.* **250**, 333–353.

Dieckmann, T., Suzuki, E., Nakamura, G. K. & Feigon, J. (1996). Solution structure of an ATP-binding RNA aptamer reveals a novel fold. *RNA*, **2**, 628–640.

Folta-Stogniew, E. & Russu, I. M. (1996). Base-catalysis of imino proton exchange in DNA: Effects of catalyst upon DNA structure and dynamics. *Biochemistry*, **35**, 8439–8449.

Forsèn, S. & Hoffman, R. A. (1963). Study of moderately rapid chemical exchange reaction by means of nuclear magnetic double resonance. *J. Chem. Phys.* **39**, 2892–2901.

Fritzsche, H., Kan, L. S. & Ts'o, P. O. P. (1983). NMR study of the exchange behaviour of the NH-N of a ribonucleic acid miniduplex. *Biochemistry*, **22**, 277–280.

Gehring, K., Leroy, J. L. & Guéron, M. (1993). A tetrameric DNA structure with protonated cytosine-cytosine base-pairs. *Nature*, **363**, 561–565.

Guéron, M. & Leroy, J. L. (1995). Studies of base-pair kinetics by NMR measurement of proton exchange. In *Methods in enzymology* (James, T. D., ed.), vol. 261, pp. 383–413, Academic Press, San Diego.

Guéron, M., Kochoyan, M. & Leroy, J. L. (1987). A single mode of DNA base-pair opening drives imino proton exchange. *Nature*, **328**, 89–92.

Guéron, M., Charretier, E., Hagerhorst, J., Kochoyan, M., Leroy, J. L. & Moraillon, A. (1989). Application of imino proton exchange to nucleic acid kinetics and structure. In *Structure and Methods, Proceedings of the Sixth Conversation in Biomolecular Stereodynamics* (Sarma, R. H. & Sarma, M. H., eds), vol. 3, pp. 113–137, Adenine Press, NY.

Jiang, F., Kumar, R. A., Jones, R. A. & Patel, D. J. (1996a). Structural basis of RNA folding and recognition in an AMP–RNA aptamer complex. *Nature*, **382**, 183–186.

Jiang, F., Fiala, R., Live, D., Kumar, R. A. & Patel, D. J. (1996b). RNA folding topology and intermolecular contacts in the AMP–RNA aptamer complex. *Biochemistry*, **35**, 13250–13256.

, Patel, D. J., Zhang, X., Zhao, H. & Jones, R. A. (1997). Specific labeling approaches to guanine and adenine imino and amino proton assignments in the AMP–RNA aptamer complex. *J. Biomol. NMR.* **9**, 55–62.

Kochoyan, M., Leroy, J. L. & Guéron, M. (1987). Proton exchange and base-pair lifetimes in a deoxy-duplex containing a purine-pyrimidine step, and in the duplex of inverse sequence. *J. Mol. Biol.* **196**, 599–608.

Kochoyan, M., Leroy, J. L. & Guéron, M. (1990). Processes of base-pair opening and proton exchange in Z-DNA. *Biochemistry,* **29**, 4799–4805.

Leontis, N. B. & Moore, P. B. (1986). Imino proton exchange in the 5 S RNA of *E. coli* and its complex with the protein L25 at 490 Mhz. *Biochemistry,* **25**, 5736–5744.

Leroy, J. L., Bolo, N., Figueroa, N., Plateau, P. & Guéron, M. (1985a). Internal motions of transfer RNA: A study of exchanging protons by magnetic resonance. *J. Biomol. Struct. Dynam.* **2**, 915–939.

Leroy, J. L., Broseta, D. & Guéron, M. (1985b). Proton exchange and base-pair kinetics of poly(rA).poly(rU) and poly(rI).poly(rC). *J. Mol. Biol.* **184**, 165–178.

Leroy, J. L., Charretier, E., Kochoyan, M. & Guéron, M. (1988a). Evidence from base-pair kinetics for two adenine tract structures in solution: their relation to DNA curvature. *Biochemistry,* **27**, 8894–8898.

Leroy, J. L., Kochoyan, M., Huynh-Dinh, T. & Guéron, M. (1988b). Characterization of base-pair opening in deoxy-duplexes, using catalyzed exchange of the imino proton. *J. Mol. Biol.* **200**, 223–238.

Leroy, J. L., Gao, X., Guéron, M. & Patel, D. J. (1991). Proton exchange and internal motions in two chromomycin dimer-DNA oligomer complexes. *Biochemistry,* **30**, 5653–5661.

Leroy, J. L., Gao, X., Misra, V., Guéron, M. & Patel, D. J. (1992). Proton exchange in DNA-luzopeptin and DNA-echinomycin bisintercalation complexes: Rates and processes of base-pair opening. *Biochemistry,* **31**, 1407–1414.

Leroy, J. L., Gehring, A., Kettani, A. & Guéron, M. (1993). Acid multimers of oligo-deoxy-cytidine strands: Stoichiometry, base-pair characterization and proton exchange properties. *Biochemistry,* **32**, 6019–6031.

Maltseva, T. V., Yamakage, S.-I. & Chattoppadhyaya, J. (1993). Direct estimation of base-pair exchange kinetics in oligo-DNA by a combination of NOESY and ROESY experiments. *Nucl. Acids Res.* **21**, 4288–4295.

Maltseva, T. V., Zarytova, V. F. & Chattoppadhyaya, J. (1995). Base-pair exchange kinetics of the imino and amino protons of the 3′-phenazinium tethered DNA-RNA duplex, r(5′-GAUUGAA-3′):d(5′-TCAATC-3′-Pzn), and their comparison with those of *B*-DNA. *J. Biochem. Biophys. Methods,* **30**, 163–177.

Moe, J. G., Folta Stogniew, E. & Russu, I. M. (1995). Energetics of base-pair opening in a DNA dodecamer containing an A3T3 tract. *Nucl. Acids Res.* **23**, 1984–1989.

Moe, J. G. & Russu, I. M. (1990). Proton exchange and base-pair opening in d(CGCGAATTCGCG) and related dodecamers. *Nucl. Acids Res.* **18**, 821–827.

Morris, G. A. & Freeman, R. (1978). Selective excitation techniques in Fourier transform NMR. *J. Magn. Res.* **29**, 433–462.

Nonin, S. (1995). Elucidation des phénomènes d'échange des protons imino de l'ADN: cas des bases modifiées, des paires terminales, et de la catalyse acide des paires G·C, Thèse de doctorat de l'Université Pierre et Marie Curie, Paris VI, .

Nonin, S. & Leroy, J. L. (1996). Structure and conversion kinetics of a bi-stable DNA *i*-motif: broken symmetry in the $[d(5mCCTCC)]_4$ tetramer. *J. Mol. Biol.* **261**, 399–414.

Nonin, S., Leroy, J. L. & Guéron, M. (1995). Terminal base-pairs of oligo-deoxynucleotides: imino proton exchange and fraying. *Biochemistry,* **34**, 10652–10659.

Nonin, S., Leroy, J. L. & Guéron, M. (1996). Acid-induced exchange of the imino proton in G·C base-pair. *Nucl. Acids Res.* **24**, 586–595.

Plateau, P. & Guéron, M. (1982). Exchangeable proton without base line distortion using a new strong pulse sequence. *J. Am. Chem. Soc.* **104**, 7310–7311.

Sassanfar, M. & Szostak, J. W. (1993). An RNA motif that binds ATP. *Nature,* **364**, 550–553.

Ts'o, P. O. P. (1974). In *Basic Principles of Nucleic Acid Chemistry,* vol. 1, pp. 462, Academic Press, New York and London.